

# Methylation detection oligonucleotide microarray analysis: a high-resolution method for detection of CpG island methylation

Sitharthan Kamalakaran<sup>1</sup>, Jude Kendall<sup>2</sup>, Xiaoyue Zhao<sup>2</sup>, Chunlao Tang<sup>2</sup>,  
Sohail Khan<sup>2</sup>, Kandasamy Ravi<sup>2</sup>, Theresa Auletta<sup>2</sup>, Michael Riggs<sup>2</sup>, Yun Wang<sup>3</sup>,  
Åslaug Helland<sup>3,4</sup>, Bjørn Naume<sup>4</sup>, Nevenka Dimitrova<sup>1</sup>, Anne-Lise Børresen-Dale<sup>3,5</sup>,  
Jim Hicks<sup>2</sup> and Robert Lucito<sup>2,\*</sup>

<sup>1</sup>Philips Research North America, Briarcliff Manor, NY 10510, USA, <sup>2</sup>Cold Spring Harbor Laboratory, Cold Spring Harbor, NY 11724, <sup>3</sup>Department of Genetics, Institute for Cancer Research, <sup>4</sup>Department of Oncology, Norwegian Radium Hospital, Rikshospitalet University Hospital and <sup>5</sup>Faculty Division, The Norwegian Radium Hospital Faculty of Medicine, University of Oslo, Oslo, Norway

Received October 9, 2008; Revised April 29, 2009; Accepted May 2, 2009

## ABSTRACT

**Methylation of CpG islands associated with genes can affect the expression of the proximal gene, and methylation of non-associated CpG islands correlates to genomic instability. This epigenetic modification has been shown to be important in many pathologies, from development and disease to cancer. We report the development of a novel high-resolution microarray that detects the methylation status of over 25 000 CpG islands in the human genome. Experiments were performed to demonstrate low system noise in the methodology and that the array probes have a high signal to noise ratio. Methylation measurements between different cell lines were validated demonstrating the accuracy of measurement. We then identified alterations in CpG islands, both those associated with gene promoters, as well as non-promoter-associated islands in a set of breast and ovarian tumors. We demonstrate that this methodology accurately identifies methylation profiles in cancer and in principle it can differentiate any CpG methylation alterations and can be adapted to analyze other species.**

## INTRODUCTION

It has become increasingly clear how epigenetic modification can affect the structure and the expression of genes encoded in the DNA. One such modification is the methylation of cytosines that are 5' to guanines, so-called CpG dinucleotides. Found scattered across the genome,

although at a lower than expected frequency, CpG dinucleotides also cluster into what have been termed CpG islands. The definition of a CpG islands differs somewhat based on the algorithm used for identification, two commonly used algorithms being Gardiner-Garden and Frommer (1) and Takai-Jones (2). The islands identified can be classified as falling into two distinct classes, those that are overlapping or proximal (within 2000 bp) to the transcription start site (TSS) of genes and those that are not associated with any transcription start site (non-TSS) for an obvious gene. Most CpG islands proximal to the TSS of genes (TSS-CGIs) are largely unmethylated normally, and methylation of these islands, as can occur during tumorigenesis, has been shown to correlate highly to the suppression of transcription (3). Of the non-TSS CpG islands (non-TSS-CGIs) in the genome, many of these are proximal or inclusive to repetitive sequences, and are generally heavily methylated in normal tissue (4,5). However, during tumorigenesis hypomethylation occurs at these islands (4,5), which can result in the expression of certain repeats (6,7). Interestingly, this hypomethylation correlates to the severity of some cancers (8,9) and DNA breakage and genome instability (10).

Under certain circumstances, which can occur in pathologies such as cancer, imprinting, development, tissue specificity and X-chromosome inactivation, TSS-CGIs can be heavily methylated (11). Specifically, in cancer, methylation of islands proximal to tumor suppressor genes such as p16, *RASSF1A*, *BRCA1*, is a frequent event (12–14). Since the analysis of such genes was previously done one at a time using bisulfite sequencing, the value of accurate high-throughput methods is obvious.

Several higher throughput methods, many array based, have been developed to identify CpG methylation in the

\*To whom correspondence should be addressed. Tel: +1 516 422 4138; Fax: +1 516 422 4109; Email: lucito@cshl.edu

genome for several different species including human and plants. An indirect approach compares expression analysis of 5-aza-cytidine treated to untreated cells (15). Early methods utilized fragments cloned from CpG island libraries (16). Illumina Inc. has developed an array-like procedure based on their bead platform (17). Several other approaches have adopted more standard array platforms utilizing DNA precipitations for human and arabidopsis with either methyl-binding proteins or antibodies that recognize methyl cytosine (ChIP-chip) (18–21). Other methods utilize methylation sensitive restriction endonucleases with or without fractionation of the genome (22–25). More recently, sequencing methods have been developed using the newest generation sequencers such as the Roche Genome Sequencer FLX (454 Lifesciences technology) (26). Although these methods are likely to replace array-based method they are presently prohibitively expensive to analyze the entire genome of large sets of samples. It is more likely that for the time being, many islands will be analyzed for few samples or few islands will be analyzed for many samples.

We have developed a method to profile genome-wide methylation that is similar to the HpaII tiny fragment Enrichment by Ligation-mediated PCR (HELP) assay (27) and MASS, which utilizes the enzyme McrBC (28), but we have made modifications to increase the methylation detection limits as well as the classes of islands analyzed. We have analyzed cell lines and validated measurements of methylation with bisulfite sequencing. We then went on to develop methods, which allow us to analyze tumors with unmatched normals, thereby accessing any samples in our tumor collection. This methodology will be useful to identify methylation events in the field of cancer as well as other fields such as development, aging, imprinting, etc.

## METHODS

### Materials

Enzymes, MspI, McrBC, T4 DNA ligase, were supplied by New England Biolabs. Primers were supplied by Sigma Genosys. Cot1 DNA and tRNA were supplied by invitrogen. The Megaprime<sup>™</sup> labeling kit, Cy3-conjugated dCTP, and Cy5-conjugated dCTP were supplied by Amersham-Bioscience. Taq polymerase [Eppendorf mastermix (2.5X)] was supplied by Eppendorf. Centricon YM-30 filters were supplied by Amicon and formamide was supplied by Amresco. Phenol:chloroform was supplied by Sigma. NimbleGen photoprint arrays were synthesized by NimbleGen Systems Inc. Design of the array was described previously (29).

### Samples

Cell lines, SKBR3, Huh7, PANC1, were acquired through ATCC and grown according to specified conditions. The cell line chp-skn-1 is a primary fibroblast cell line cultured from a skin sample provided by an anonymous donor, cultured under the following conditions: DMEM + 20% FBS, Penn/Strep, and non-essential amino acids. Tumor DNA from 11 patients with advanced ovarian carcinomas

who were treated at the Department of Gynecological Oncology at The Norwegian Radium Hospital (NRH) during the period May 1992 to February 2003 were included in this study. The collection is approved by the Regional ethical review board (Reference No: S-01127). Tumor DNA from 28 patients treated for localized breast cancer at the Norwegian Radium Hospital (NRH) from 1995 to 1998 was included in this project. The samples were collected under an informed consent and the project approved by the local REK/IRB (30). A small number of samples 12 breast tumors and 12 normals and 7 ovarian normals were obtained from The Cooperative Human Tissue Network, a repository of tumor material run by the National Institutes of Health.

### Methylation array and detection

**Coverage.** Our approach to map genome-wide methylation involves tiling all the predicted CpG islands. All annotated CpG islands were obtained from the UCSC genome browser. These islands were predicted using the published Gardiner-Garden and Frommer (1) definition and involves the following criteria: length  $\geq 200$  bp, %GC  $\geq 50\%$ , observed/expected CpG  $\geq 0.6$ . There are  $\sim 26219$  CpG islands in the range of 200–2000 bp in the genome. These islands are well covered by Msp I restriction fragmentation. Arrays were manufactured by Nimblegen Systems Inc. using the 390K format to the following specifications. The CpG island annotation from human genome build 33 (hg17) was used to design a 50-mer tiling array. The 50 mers were shifted on either side of the island sequence coordinates to evenly distribute the island. The 390K format has 367658 available features which would not fit all islands with a 50-mer tiling. Therefore, we made a cutoff on the islands to be represented based on size, with only CpG islands of size 200–2000 bp being assayed. The array represents classical CpG islands and does not include imprint control regions or other non-island promoters known to be methylated. Background hybridization signal could be high with probes of high GC content since by definition these probes will be. Therefore, control probes, which are not in an MspI representation, were designed to represent background signal, and these probes were used to calculate signal to noise (see Supplementary Figure 2). Array design, probe sequences and further annotation are available on line <http://www.ncbi.nlm.nih.gov/geo/>, dataset number GSE15801.

### Sample preparation and hybridization

Representations have been described previously (29), with the following changes. The primary restriction endonuclease used is MspI. After the digestion the following linkers were ligated (MspI24mer CAGCATCGAGACTGACGCAGCAG, and MspI12mer CGCTGCTGCGTT). The 12 mer is not phosphorylated and does not ligate. After ligation the material is cleaned by phenol chloroform, precipitated, centrifuged and resuspended. The material is divided in two, half being digested by the endonuclease McrBC and the other half being mock digested according to specification by New England Biolabs.

The digestion time is 3 h. As few as four 250  $\mu$ l tubes were used for each sample pair for amplification of the representation each with a 100  $\mu$ l volume reaction. The cycle conditions were 95°C for 1 min, 72°C for 3 min, for 15 cycles, followed by a 10-min extension at 72°C. The contents of the tubes for each pair were pooled when completed. Representations were cleaned by phenol:chloroform extraction, precipitated, resuspended and the concentration determined. Representations were run on a gel to check for content, the McrBC digested representation being ~100–150 bp shorter on average than the Mock. DNA was labeled as described with minor changes (29). Briefly, 2  $\mu$ g of DNA template was placed (dissolved in TE at pH 8) in a 0.2 ml PCR tube. Five microliters of random nonomers (Sigma Genosys) were added brought up to 25  $\mu$ l with dH<sub>2</sub>O, and mixed. The tubes were placed in Tetrad at 100°C for 5 min, then on ice for 5 min. To this 5  $\mu$ l of NEB Buffer 2, 5  $\mu$ l of dNTPs (0.6 mM dCTP, 1.2-mM dATP, dTTP, dGTP), 5  $\mu$ l of label (Cy3-dCTP or Cy5-dCTP) from GE Healthcare, 2  $\mu$ l of NEB Klenow fragment and 2  $\mu$ l dH<sub>2</sub>O were added. Procedures for hybridization and washing were followed as reported previously (29) with the exception that oven temperature for hybridization was increased to 50°C. In general two hybridizations were performed for all samples (carried out as dye swaps to decrease variation of labeled nucleotide incorporation) with the exception for samples analyzed in Figure 2 where four hybridizations were performed.

#### Data analysis and statistics

Microarray images were scanned on GenePix 4000B scanner and data extracted using NimbleScan software (Nimblegen Systems Inc.). For each probe, the geometric mean of the ratios (GeoMeanRatio) of McrBc and control treated samples were then calculated for each experiment and its associated dye swap. The GeoMeanRatios of all the samples in a dataset were then normalized using quantile normalization method (31). The normalized ratios for each experiment were then collapsed to get one value for all probes in every MspI fragment using the median polish model. The collapsed data were then used for further analysis (32). Collapsed fragment data were then subjected to Welch's two-sample *t*-test for identifying significant differences between tumors and normals. *P*-values were corrected for multiple testing by controlling false discovery rate (FDR) (Benjamini-Hochberg algorithm) (33) implemented in R [multitest package (34)]. Significance threshold was set at 0.001 for breast and 0.05 for the smaller ovarian set.

General computations and statistics were performed in Python (35), S-Plus and R (32).

#### Bisulfite sequencing

Probes were identified with differing methylation between the two samples, SKBR3 and chp-skn-1. DNAs from the two samples were treated with bisulfite using the EZ DNA Methylation-Gold Kit (Zymo Research, CA, USA). PCR primers were designed to flank the corresponding MspI fragments using MethPrimer (36). For two fragments, the PCR-amplified fragments were ligated

and transformed using the TOPO-TA Cloning kit (Invitrogen, CA, USA); the transformant clones were picked for plasmid extraction, which were then sequenced. To increase throughput, the remaining 32 were sequenced as PCR products. Results for subcloning and direct sequencing were compared to determine the peak heights required to call heterozygotes.

#### McrBC PCR

The sequence of the MTSS1 CpG island was obtained, including sequence beyond the ends of the island to aid in the design of PCR primers. Genomic DNA was digested with McrBC or mock digested followed by heat killing. Ten nanograms of DNA was used for PCR with Qiagen Taq polymerase for 30 cycles. Ten microliters of this product was then used as template for an additional 15 cycles of PCR. Products were run on 2% agarose gel, and pictures were taken to illustrate the fragments that were methylated.

## RESULTS

In order to further investigate the role that CpG island methylation plays in cancer, we have designed a new comprehensive CpG island microarray and have developed robust methods for its use. While sharing some similarities to previously developed methylation arrays (22,27,37), our method has several features that allow for increased CpG-island coverage and sensitivity. First, we utilized high-density oligonucleotide arrays with close to 400K features that allowed us to maximize tiling coverage of 26 219 out of 27 801 (HG17) annotated CpG islands (which includes non-promoter islands), while other CpG island arrays only contain selected promoter sequences (22,37). Second, our hybridization target, because it is made from MspI representations, enriches for CpG island sequences by 10-fold relative to total genomic DNA (based on the size or the MspI amplifiable fragment) and thus provides superior hybridization specificity. In addition since this method is representational based, very little DNA is required (as little as 50 ng) which makes this method well suited to the analysis of primary tumors. Third, each island generally corresponds to multiple MspI fragments, yielding positional information of which portion of an island is methylated. Finally, our method is based on enzymatic depletion of methylated sequences with fewer steps than other methods (37,38); having fewer steps may be less prone to variability. The enzyme chosen for depletion, McrBC, has the unusual recognition site A/GC<sup>m</sup>(N<sub>40–3000</sub>)A/GC<sup>m</sup> and has been used by others to analyze methylation including its application to arrays (39,40). This enzyme recognizes two methyl groups and because of the varied distance and that the methyl groups can be on the same or both strands (41), a type of combinatorial recognition and cleavage occurs, which greatly increases the number of potentially methylated CpG dinucleotides that can be queried. Using *in-silico* analysis we calculate using McrBC (specifically the preferred distance for recognition between methyl cytosines of 40–150 bp) our methodology queries over



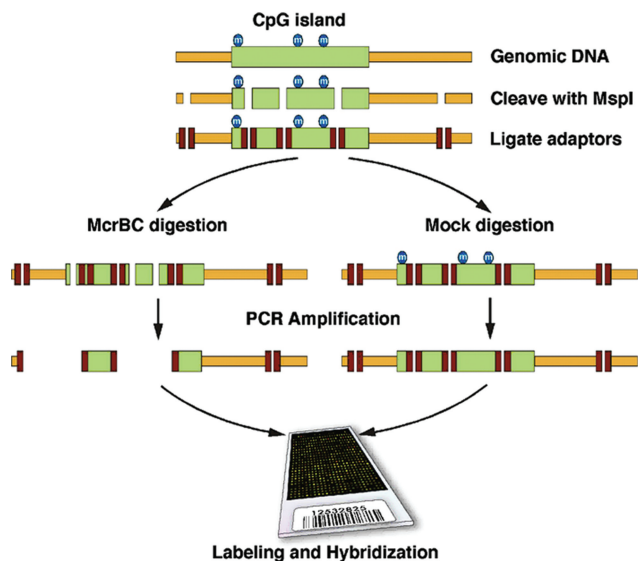


**Figure 1.** Schematic of the procedure. Shown at the top is genomic DNA with a CpG island that is methylated. The DNA is cleaved with the restriction endonuclease MspI and adaptors ligated. The ligated material is divided evenly, one half being digested with McrBC and the other half being mock digested. This material is used as template for PCR amplification and the resulting product is used for microarray comparison.

1 million of the 1.7 million CpG dinucleotides occurring in CpG islands, much more than can be queried by other techniques that utilize different enzymatic depletions such as HpaII and MspI (~225 000). This gives our methodology a 4-fold increase in potential coverage over other methods. According to these calculations combined with the increased array coverage (where we include non-promoter sequences and do not discriminate against any other promoter sequences except for larger islands, see ‘Methods for array design’ section) we will have increased the level of DNA methylation that can be measured in the genome over other methods which either use restriction enzymes or limited array coverage (data not shown).

The procedure as schematized in Figure 1 involves digesting the genome with a restriction endonuclease with a CG-rich recognition sequence (MspI), and ligation of adaptors for use in a subsequent step of reducing genomic complexity. We next divide the ligation in half and deplete one-half of its methylated sequences by digestion with the methylation-specific endonuclease, McrBC (37), and mock treat the other half. In both cases, we use carefully balanced PCR conditions to size select MspI fragments and reduce the overall genome complexity as previously described (29). The McrBC-treated representation is compared to the mock-treated sample that serves as the reference for comparative hybridization to the designed oligonucleotide array.

To determine if our method accurately identifies the methylation state of CpG islands, we first performed initial experiments with cell lines. To determine the level of noise in the system we performed analysis on a normal fibroblast cell line (chp-skn-1). Two cultures of chp-skn-1 were grown and DNA prepared. Representations were

prepared and were used to compare hybridization results from the same representations, representation from the same sample prepared separately, as well as the chp-skn-1 grown separately. Generally two hybridizations are performed one being a dye swap to decrease variation but in this case four hybridizations were performed for all conditions; however to demonstrate how little noise there is in the system, results and correlation from a single hybridization were compared graphically shown in Figure 2A–C. The close correlation demonstrates the small variation in the representational process, the labeling and the hybridization. We also found little variation among different lots of McrBC (data not shown). Included on the array are probes that are not in a representation but have moderate CpG density. Using the average intensity for these probes in the mock channel as the background component we measured signal to noise for the probes on the array. The average signal to noise for probes on the array was 10.39.

We then performed a comparison of the breast cancer cell line SKBR3 with chp-skn-1, shown in Figure 2D (with a correlation of 0.831, which demonstrates that there are differences detected between two different samples as compared to the control experiments shown in Figure 2A–C. In the scatter plot (Figure 2D), points off the central diagonal represent fragments detecting differential methylation between the two samples. To evaluate the accuracy of measurements 25 fragments identified with methylation differences between chp-skn-1 and SKBR3, and nine fragments with no detection of methylation were selected for validation by sodium bisulfite sequencing (42). Analysis of one representative fragment is shown in Figure 2E. In each of the 28 fragments sequenced CpG dinucleotides inclusive of McrBC sites were mapped and their methylation state identified in the two samples (Supplementary Figure 1 for five non-gene islands, five non-CpG island regions and 10 gene-associated islands; Supplementary Table 1 which has data for all 28 fragments). Fragments were selected based on varying the difference in the array ratios measured for both samples. By doing so we were able to determine at what level accurate measurements of methylation can be determined. At a difference around 0.3 the measurements may be incorrect as can be seen by two fragments, which had a difference in ratio of 0.317. Any ratio difference above this level was found to be methylated in one of the samples. To determine if our method could accurately identify known tumor suppressor CpG island methylation, we then analyzed the hepatocellular cancer cell line HuH7 with known methylation of the p16 promoter (43). In Figure 2F we show the detection of methylation of the region of the p16 gene CpG island commonly methylated and correlated with decreased gene transcription.

Finally, we compared the results of our methodology on the two cell lines HPDE and PANC1 with results from the same two cell lines reported by Sato and colleagues using a different method and different array design (44). Although there were some differences in detection between the two methods they were in good agreement (68%) for islands methylated in the samples. Of the 34 interesting islands listed and validated, 26 were represented on our array

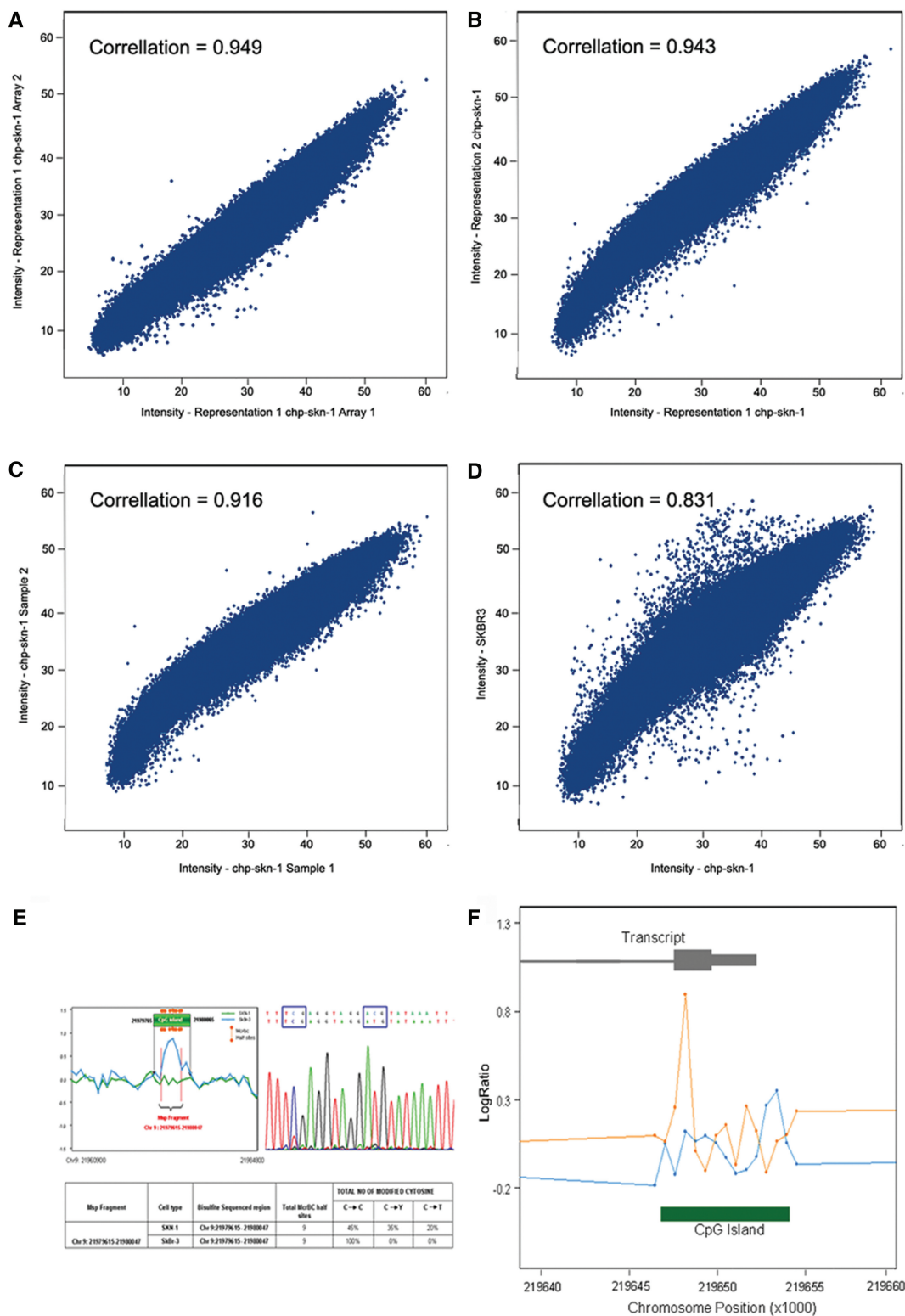


**Figure 2.** Comparison of methylation analysis of cell lines. (A–C) shows the comparison of a normal fibroblast used to produce representations from two separate aliquots of DNA and the representations were analyzed and the intensity compared to each other by scatter plot; the intensities of each being on one and the other axis, and the correlation calculated: (A) being replicate hybs, (B) being technical replicates and (C) being biological replicates. (D) The comparison of the breast cancer cell line SKBR3 and the normal female fibroblast cell line as a scatter plot of the intensities from the SKBR3 experiment as the y-axis and the intensities of chp-skn-1 on the x-axis, and the correlation shown. (E) An example of bisulfite validation for a fragment found methylated in the tumor and not in the normal at a CpG island at chr 9:2197965–2198065, which lies upstream of the p14 gene. The original data showing the ratio differences is shown with the position of the fragment. To the right is the electropherogram identifying a region of cytosines that do not convert and at the bottom is a short table identifying the genomic position and number of MspBC site. (F) shows data for the cell line Huh7 compared to the normal cell line chp-skn-1 for the p16 gene CpG island graphed by genomic position. The x-axis is the genomic position of the probes and the y-axis is the ratio of two experiments, blue being chp-skn-1 and orange being Huh7. Inset above is shown is the relation of the transcript and inset below is the relation of the CpG island to the probes.

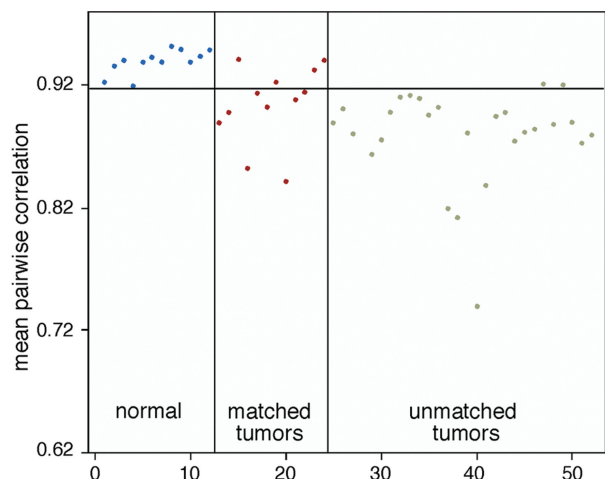


**Figure 3.** The mean correlation for each sample with the normal samples (mean of 12 correlations for each tumor and 11 correlations for each normal) is shown. The 12 samples to the left of the vertical line are the normals. The 40 to the right are tumors. The horizontal line is drawn at the minimum mean correlation for the normals with normals. It is apparent that the tumors are on the whole distinct from the normals in comparison with each other ( $P < 10E-017$ ).

(Supplementary Table 2, panel A). Of the 26, 17 regions were properly identified with methylation in PANC1 or both. Four regions identified as methylated by Sato and colleagues were not detected in our assay. There was disagreement in four regions. One gene *RELN*, which was reported as not methylated in either sample by Sato and colleagues, was found methylated in PANC1 cells. Interestingly, this gene is frequently methylated and silenced in pancreatic tumors (45), suggesting that our cell line may have genetically drifted over time apart from that used by Sato and colleagues. With our method we can obtain positional information for the region of the CpG island methylated and for all methylation events the region is very close to the TSS, the region critical for suppression of transcription. To determine the accuracy of methylation detection as well as the positional prediction we performed sodium bisulfite sequencing on the fragment, which was detected as methylated in the *RELN* CpG island in the PANC1 cell line. Interestingly, we found that the CpG island fragment at position chr7:103223731–103223823 is methylated (Supplementary Table 2, panel B) demonstrating that the method can accurately identify methylation and that positional information is also available. In addition we have determined that our line of PANC1 cells has deviated from the line used by SATO and colleagues.

The standard method to analyze tumor-methylation profiling is to utilize matched normal-tumor samples, and we have done this for 12 breast tumor and normal pairs. As with many tumor banks, ours contain many unmatched tumor samples. To determine if unmatched tumor-normal pairs could be analyzed first we compared our results obtained with matched samples to those obtained with unmatched samples as a set and measured

the degree of common alterations. We developed statistical criteria for identifying CpG-islands most significantly altered between tumor and normal (see ‘Methods for details’ section). Our analysis identified considerable overlap (30%) of CpG-islands significantly altered (Supplementary Table 3) between a matched tumor-normal set (12 normals, 12 tumors) compared to an unmatched set (12 normals, 28 tumors). Since all tumor samples are different, similarity among a set could be a measure of tumor selection. We determined how different all 40 tumors were from the normal samples. We computed pair-wise correlations between each normal sample and the other normals and each tumor sample to each normal. From this data we then computed the mean correlation between each sample and the normal samples. The mean correlation from normals to normals is 0.93, from tumors to normals is .88 ( $P < 10E-017$ ). These data (plotted in Figure 3) show that tumors are different from matched or unmatched normals. However, while some tumors are vastly different from normal several are more normal like in their methylation profile. In the future it will be interesting to have more detailed clinical information to determine if methylation profile can determine specific clinical parameters. Thus, we moved on to the analysis of a larger set of unmatched tumors and normals.

We then examined the set of 40 breast tumors, compared to 12 normal breast samples and 11 ovarian tumors compared to 7 normal ovarian samples (33). Using the statistical criteria developed (detailed in the ‘Methods’ section) we obtained a list of 916 significant alterations in breast cancer and 151 in ovarian cancer and have listed these by their genomic location (see Supplementary Table 4 for entire list and Table 2 for a summary of whether the alterations were found with more methylation or less methylation than normal, based on specific classes, non-promoter associated or promoter associated as well as non-island regions). In Table 1 we highlight genes selected based on functional information, many of which have previously been documented to alter methylation in cancer again demonstrating the ability of this methodology to detect CpG methylation. Genes identified hypermethylated in both ovarian and breast tumors include several *HOX* genes and protocadherins, known to be methylated in many tumor types (46–49). In addition to genes known to undergo methylation we have found new targets of methylation. For example, we detected for promoter methylation of a micro-RNA gene *has-mir-9-3*, occurring in more than half the breast tumors. This miRNA has been shown to be downregulated transcriptionally in thyroid cancers (50).

Another gene identified as methylated in the breast tumors, *MTSS1* (metastasis suppressor 1) (Table 1) is known to be preferentially methylated in several cancers including breast cancer (51–53). To determine if our analytical methods identified this gene accurately, two primary tumors were identified with methylation from the dataset for further validation. Being that they were not cell lines we only had 25 ng of material that we wanted to check multiple times. Although bisulfite sequencing is generally used for validation we wished to use an alternative due to the small amount of genomic DNA remaining.



**Table 1.** Short list of genes selected from Supplementary Table 4 with altered CpG islands<sup>a</sup>

GeneName	Name	Location	Importance
<b>Methylated</b>			
EPHA2	Ephrin receptor A2	chr1_16196139_16227870	With E cadherin, mult roles in cancer
HOXD11	Homeodomain protein	chr2_176795292_176795763	Development and differentiation
HOXD9	Homeodomain protein	chr2_176807548_176807855	Development and differentiation
PPM1G	Protein phos'tase 1G	chr2_27544151_27545066	Cell cycle progression
RAB6B	Ras oncogene family	chr3_135097550_135098100	G protein regulation of proliferation
MF12	Melanoma-associated Ag 2	chr3_198245561_198245644	Melanoma tumor progression
IL17RB	Interleukin 17 receptor B	chr3_53855151_53855185	With HOXB13 progression in breast cancer
HHIP	Hedgehog interacting protein	chr4_145923993_145924160	Metastasis in panc cancer
SFRP2	Secreted frizzled related protein 2	chr4_155067811_155068195	Methylated is marker for colon cancer
CRMP1	Collapsin response mediator prot 1	chr4_6010436_6010699	Wnt pathway, lung met suppression
PKD2	Polycystic kidney disease 2	chr4_89285337_89285745	Cell cycle
PCDHGA10	Protocadherin gamma, subfam A	chr5_140768066_140768556	Cell adhesion
HOXA2	Homeodomain protein	chr7_26919212_26919376	Development and differentiation
HOXA3	Homeodomain protein	chr7_26942376_26942852	Development and differentiation
EPDR1	Ependymin related protein 1	chr7_37728939_37729281	Ca <sup>++</sup> dependent cell adhesion
TAC1	Tachykinin, precursor 1	chr7_97005815_97006071	Inflam prohormones; low act'y in brst cncr
MTSS1	Metastasis suppressor 1	chr8_125810238_125810819	Metastasis suppressor
TNFRSF10D	Tumor necrosis factor superfamily	chr8_23077244_23077520	Progression neuroblastoma/breast cancer
CUGBP1	CUG triplet rpt, RNA bind prot	chr11_47531208_47531279	Reg p21, cell cycle control
NFYB	Nuc. transcr. fctr Y beta	chr12_103034912_103035336	p53 cell cycle
*PCDH8	Protocadherin 8	chr13_52320446_52320832	Cell adhesion
ONECUT1	Onecut homeobox domain 1	chr15_50874380_50874668	Reg.expression of FOXA2
CDH8	Cadherin 8, type 2	chr16_60627191_60627579	Cell adhesion; freq deleted in brst cncr
PPP1R14A	Protein phos'tase 1 reg subunit 14A	chr19_43439132_43439444	Reg act'y RAS and ERK in tumor lines
IL28A/B	Interleukin 23 interferon like	chr19_44447259_44447674	Inhibit tumor proliferation
FOXA2	Forkhead box A2	chr20_22514937_22515431	Lung/prostate cancer
PLCG1	Phospholipase C gamma 1	chr20_39198472_39198934	Implicated in cancer and metastatsis
RTEL1	Regulator telemere elong.helicase	chr20_61758790_61759467	Req for telomer elong.; chr breaks/loss
PRR5	Proline rich 5 (renal)	chr22_43445548_43445907	Downreg in breast cancer
SHOX	Short stature homeobox	chrX_551021_551222	Reg of proliferation and viability
<b>Demethylated</b>			
BRDT	Bromo domain prot testis spec.	chr1_92126308_92126790	Spermatogenesis
RRM2	Ribonucleotide reductase M2	chr2_10212057_10212966	Chemotherapy target
BCL11A	B cell lymphoma protein 11A	chr2_60694090_60694350	Cofactor w/ SIRT1 in transcrip'n regulation
DUB3	Deubiquinating enzyme 3	chr4_9040795_9041453	Proliferation
RHOG	Ras homolog gene family G	chr11_3819507_3820119	Apoptosis, migration
SULT1A1	Sulfotransferase family	chr16_28542367_28542407	Response to therapy and prog. brst cancer
BECN1	BCL2 interacting protein	chr17_38229845_38229898	Multiple roles in cancer
STRA13	Stimulated by retinoic acid 13	chr17_77574908_77575250	Role in cell cycle and carcinogenesis
MAPK1	Map kinase 1/ERK	chr22_20546877_20547317	Proliferation

<sup>a</sup>Genes of possible functional interest were tabulated from the two categories based on TSS association. The gene abbreviation, full gene name, fragment location, and description of the gene are given.

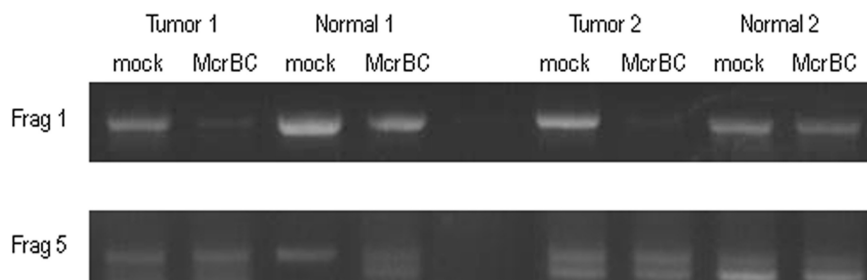


**Figure 4.** McrBC PCR of two different fragments of the MTSS1 CpG island for tumors identified of having methylation of this island compared to matched normal samples. Fragment 1 encompasses the MspI fragment we have identified as being methylated and overlaps the gene TSS. Fragment 5, we do not detect methylation. Both Normal and Tumor were digested with McrBC or mock digested for both matched pairs.

Others have utilized McrBC combine with PCR to study methylation (39,54). Due to the constraints on us we chose to perform McrBC PCR (40) to validate the region of the island detected as methylated (Figure 4). The island was broken down into five fragments where fragment one

overlaps the TSS up to fragment five that is the farthest away from the TSS. For tumors that were suspect to have methylation, fragment 1, which overlaps the gene TSS could not be amplified in the tumor samples (due to digestion by McrBC demonstrating methylation) as

**Table 2.** Summary of significant methylation changes listed in Supplementary Table 4 for breast cancer<sup>a</sup>

	TSS associated (%)			Non-TSS associated (%)		
	Methylated	Demethylated	Total	Methylated	Demethylated	Total
CGI (801)	166 (77.93)	47 (22.07)	213	517 (87.92)	71 (12.07)	588
Non CGI (115)	3 (33.33)	6 (66.64)	9	23 (21.70)	83 (78.30)	106

<sup>a</sup>All methylation and demethylation events from Supplemental Table 4 were broken down into categories of associated to a gene (TSS associated) or not (Non-TSS associated), and methylated or demethylated within each of these groups. Finally the probes are divided based on inclusiveness to a CpG island or the probes that are non-CGI probes. The total number is given for breast cancer comparison as well as the conversion to percentages in parentheses.

compared to the normal, which was not digested by McrBC (no methylation). Fragment 5 that is far from the TSS is amplified in all samples including McrBC digested due to a lack of methylation and no cleavage by McrBC, demonstrating that the *MTSS1* CpG island is methylated in primary tumors.

## DISCUSSION

We have designed a methylation array and developed methods to detect CpG methylation. This methodology was performed on cell lines and measurements validated with more standard methods. Comparing the analysis of two cell lines by our methodology allowed us to test the accuracy by bisulfite sequencing fragments with differential methylation between the two cell lines. We found no errors except for one fragment that was methylated but was not detected. This could have been a failure of the McrBC or the array detection. We suspect the oligonucleotide probe since as in all hybridization-based method, there are bound to be probes that do not report well. In comparison of our method with another array-based methods for the analysis of the same samples, we found good correspondence between the two methods. One gene we found particularly interesting, *RELN*, is frequently silenced in pancreatic cancer. Sato and colleagues demonstrate that it is not methylated in this particular pancreatic cancer cell line but our measurements suggest that it is methylated. Judging from its frequency of silencing and our success in validation of our measurements it is likely that our version of the cell line has genetically, or in this case, epigenetically drifted from that used by Sato and colleagues. To determine if this was the case we validated our findings by bisulfite sequencing and determined that our version of the cell line had deviated and the array was correct in its measurement.

In our analysis of tumors versus normal, as expected, the tumors had more variation than the normals. However, some tumors were remarkably similar while others very different from their matched normal. More importantly, the unmatched tumors were for the most part similar in variation to normal as the matched tumors. Three breast tumors out of 40 and 2 ovarian tumors out of 11 were extremely different from the normals, which could be interesting in reference to clinical parameters or genome structure and we are investigating this further with sample sets of a larger size. We then developed statistical methods that could be used to

identify those CpG islands that differ in their methylation status in the tumors as compared to the normals.

We have identified a number of CpG islands, both associated with gene TSSs or islands far from the TSS for any genes, which have altered methylation from both breast and ovarian tumors as compared to normal. However, we did not identify well-known tumor suppressors in the primary tumor dataset such as *p16*. The lack of known tumor suppressors could be a fault in our analysis or our methods. However, the frequency of methylation for many classically known tumor suppressors varies widely, some being as low as 15% (55–58). Using *p16* as an example, analysis of the tumor samples with matched normals did not uncover tumor suppressors such as *p16* and since we demonstrate the ability to detect *p16* methylation in the cell line HuH7 (43) with known methylation it is likely that none of the tumors had methylation of *p16*. Therefore, although improvements are always possible, we feel that our technical and analytical methods are sound. Unfortunately, the tumor suppressor *Rassf1a* that is a common target of methylation in cancer is not measurable with the current array. The next generation array will include better design of CpG islands such as those proximal to the *Rassf1A*.

One disadvantage of our method of analysis is that those genes whose CGIs are found with altered methylation in few samples may not be identified. The MiR-196 loci on chromosome 17 is methylated in several of the breast cancers in our study as compared to matched normals but overall is not significant in the larger set. It has been previously shown that the miR-196 directs the cleavage of *HoxB8* mRNA (59), which appears to function in myeloid differentiation (60,61), however it is possible that it plays a role in the deregulation of breast cells in becoming cancer. Presently we are further developing our statistical methods to improve our level of detection.

Of the islands associated with gene TSSs identified as methylated there are a number that have been found altered and/or have been shown by other to decrease in expression in cancer, such as *MTSS1* (51–53). We found this island methylated in a number of the primary breast tumors and verified by McrBC PCR (54) that it was methylated in two of these (one such sample shown in Figure 4). Tumor suppressors that are methylated are often found in regions of loss of heterozygosity (LOH). It will be interesting to determine which of the genes found methylated are in regions of LOH. It is interesting that *MTSS1* is found on the q arm of chromosome 8, which is



amplified very frequently in breast cancer and ovarian tumors. It is possible that *MTSS1* loss is important to the tumor growth as suggested by its role in cytoskeletal rearrangement (62) and its correlation with the disease state (51), so that in order to ensure lack of transcription within a region of genomic amplification the gene is silenced by methylation. It will be interesting to associate CGH data with methylation data and incorporate expression analysis to identify genes that are methylated and suppressed and determine if they are amplified or deleted genomically.

Of the genes identified, those that are functionally interesting should have their methylation validated by other means such as bisulfite sequencing or MCRBC PCR. Those that pass can be functionally validated as candidates with possible tumor-suppressive activity. In conclusion, we have developed a powerful method to profile genome-wide DNA methylation. We have demonstrated that there is very low system noise from either the representational process or the labeling and hybridization. We then legitimized the method's ability to detect methylation by bisulfite sequence validating over 15 fragments. We went on to analyze a number of samples that have been analyzed by others either by bisulfite sequencing or by other genome-wide approaches for methylation detection (43,45). In the case of Maeta *et al.*, we have validated specific methylation events and in the case of Sato *et al.* we have reproduced the majority of their findings using our methodology. We then used this method to develop methods for the analysis of tumors with unmatched normals, which will be of interest to the greater community since many tumor banks do not have matched normals. We plan on using this methodology to identify methylation events that correlate to clinical parameters to determine if tumor sub-classification can be achieved, markers from this type of analysis being very valuable. In addition, this methodology will have utility in the study of other pathologies, such as imprinting, development, or tissue specificity, which all are affected by epigenetic modifications.

## SUPPLEMENTARY DATA

Supplementary Data are available at NAR Online.

## ACKNOWLEDGEMENTS

We thank Scott Powers, Scott Lowe, Michael Wigler and Michael Zhang for critical comments on the manuscript. We also thank Christopher Johns for assistance in design of the arrays. Some tumor samples were supplied by the Cooperative Human Tissue Network, which is funded by the National Cancer Institute. Other investigators may have received samples from these same tissues.

## FUNDING

National Institutes of Health and National Cancer Institute [K01CA93634-01 to R.L.]; Department of Defense [W81XWH-05-1-0068 to R.L.] as well as by grants awarded to Michael Wigler from the Simons

Foundation and the Breast Cancer Research Foundation. Funding for open access charge: awarded to RL and Michael Wigler from Philips Research North America.

*Conflict of interest statement.* None declared.

## REFERENCES

- Gardiner-Garden, M. and Frommer, M. (1987) CpG islands in vertebrate genomes. *J. Mol. Biol.*, **196**, 261–282.
- Takai, D. and Jones, P.A. (2002) Comprehensive analysis of CpG islands in human chromosomes 21 and 22. *Proc. Natl Acad. Sci. USA*, **99**, 3740–3745.
- Herman, J.G. and Baylin, S.B. (2003) Gene silencing in cancer in association with promoter hypermethylation. *N. Engl. J. Med.*, **349**, 2042–2054.
- Baylin, S.B., Herman, J.G., Graff, J.R., Vertino, P.M. and Issa, J.P. (1998) Alterations in DNA methylation: a fundamental aspect of neoplasia. *Adv. Cancer Res.*, **72**, 141–196.
- Bird, A.P. (1996) The relationship of DNA methylation to cancer. *Cancer Surv.*, **28**, 87–101.
- Lavie, L., Kitova, M., Maldener, E., Meese, E. and Mayer, J. (2005) CpG methylation directly regulates transcriptional activity of the human endogenous retrovirus family HERV-K(HML-2). *J. Virol.*, **79**, 876–883.
- Roman-Gomez, J., Jimenez-Velasco, A., Agirre, X., Cervantes, F., Sanchez, J., Garate, L., Barrios, M., Castillejo, J.A., Navarro, G., Colomer, D. *et al.* (2005) Promoter hypomethylation of the LINE-1 retrotransposable elements activates sense/antisense transcription and marks the progression of chronic myeloid leukemia. *Oncogene*, **24**, 7213–7223.
- Cho, N.Y., Kim, B.H., Choi, M., Yoo, E.J., Moon, K.C., Cho, Y.M., Kim, D. and Kang, G.H. (2007) Hypermethylation of CpG island loci and hypomethylation of LINE-1 and Alu repeats in prostate adenocarcinoma and their relationship to clinicopathological features. *J. Pathol.*, **211**, 269–277.
- Smith, I.M., Mydlarz, W.K., Mithani, S.K. and Califano, J.A. (2007) DNA global hypomethylation in squamous cell head and neck cancer associated with smoking, alcohol consumption and stage. *Int. J. Cancer*, **121**, 1724–1728.
- Ehrlich, M. (2002) DNA hypomethylation, cancer, the immunodeficiency, centromeric region instability, facial anomalies syndrome and chromosomal rearrangements. *J. Nutr.*, **132**, 2424S–2429S.
- Bird, A. (2002) DNA methylation patterns and epigenetic memory. *Genes Dev.*, **16**, 6–21.
- Merlo, A., Herman, J.G., Mao, L., Lee, D.J., Gabrielson, E., Burger, P.C., Baylin, S.B. and Sidransky, D. (1995) 5' CpG island methylation is associated with transcriptional silencing of the tumour suppressor p16/CDKN2/MTS1 in human cancers. *Nat. Med.*, **1**, 686–692.
- Dammann, R., Li, C., Yoon, J.H., Chin, P.L., Bates, S. and Pfeifer, G.P. (2000) Epigenetic inactivation of a RAS association domain family protein from the lung tumour suppressor locus 3p21.3. *Nat. Genet.*, **25**, 315–319.
- Rice, J.C., Massey-Brown, K.S. and Futscher, B.W. (1998) Aberrant methylation of the BRCA1 CpG island promoter is associated with decreased BRCA1 mRNA in sporadic breast cancer cells. *Oncogene*, **17**, 1807–1812.
- Shames, D.S., Minna, J.D. and Gazdar, A.F. (2007) DNA methylation in health, disease, and cancer. *Curr. Mol. Med.*, **7**, 85–102.
- Estecio, M.R., Yan, P.S., Ibrahim, A.E., Tellez, C.S., Shen, L., Huang, T.H. and Issa, J.P. (2007) High-throughput methylation profiling by MCA coupled to CpG island microarray. *Genome Res.*, **17**, 1529–1536.
- Bibikova, M., Lin, Z., Zhou, L., Chudin, E., Garcia, E.W., Wu, B., Doucet, D., Thomas, N.J., Wang, Y., Vollmer, E. *et al.* (2006) High-throughput DNA methylation profiling using universal bead arrays. *Genome Res.*, **16**, 383–393.
- Weber, M., Davies, J.J., Wittig, D., Oakeley, E.J., Haase, M., Lam, W.L. and Schubeler, D. (2005) Chromosome-wide and promoter-specific analyses identify sites of differential DNA

- methylation in normal and transformed human cells. *Nat. Genet.*, **37**, 853–862.
19. Ballestar, E., Paz, M.F., Valle, L., Wei, S., Fraga, M.F., Espada, J., Cigudosa, J.C., Huang, T.H. and Esteller, M. (2003) Methyl-CpG binding proteins identify novel sites of epigenetic inactivation in human cancer. *EMBO J.*, **22**, 6335–6345.
  20. Zhang, X., Yazaki, J., Sundaresan, A., Cokus, S., Chan, S.W., Chen, H., Henderson, I.R., Shinn, P., Pellegrini, M., Jacobsen, S.E. *et al.* (2006) Genome-wide high-resolution mapping and functional analysis of DNA methylation in arabidopsis. *Cell*, **126**, 1189–1201.
  21. Zilberman, D., Gehring, M., Tran, R.K., Ballinger, T. and Henikoff, S. (2007) Genome-wide analysis of Arabidopsis thaliana DNA methylation uncovers an interdependence between methylation and transcription. *Nat. Genet.*, **39**, 61–69.
  22. Adrien, L.R., Schlecht, N.F., Kawachi, N., Smith, R.V., Brandwein-Gensler, M., Massimi, A., Chen, S., Prystowsky, M.B., Childs, G. and Belbin, T.J. (2006) Classification of DNA methylation patterns in tumor cell genomes using a CpG island microarray. *Cytogenet. Genome Res.*, **114**, 16–23.
  23. Balog, R.P., de Souza, Y.E., Tang, H.M., DeMasellis, G.M., Gao, B., Avila, A., Gaban, D.J., Mittelman, D., Minna, J.D., Luebeck, K.J. *et al.* (2002) Parallel assessment of CpG methylation by two-color hybridization with oligonucleotide arrays. *Anal. Biochem.*, **309**, 301–310.
  24. Hatada, I., Fukasawa, M., Kimura, M., Morita, S., Yamada, K., Yoshikawa, T., Yamanaka, S., Endo, C., Sakurada, A., Sato, M. *et al.* (2006) Genome-wide profiling of promoter methylation in human. *Oncogene*, **25**, 3059–3064.
  25. Yan, P.S., Perry, M.R., Lau, D.E., Asare, A.L., Caldwell, C.W. and Huang, T.H. (2000) CpG island arrays: an application toward deciphering epigenetic signatures of breast cancer. *Clin. Cancer Res.*, **6**, 1432–1438.
  26. Taylor, K.H., Kramer, R.S., Davis, J.W., Guo, J., Duff, D.J., Xu, D., Caldwell, C.W. and Shi, H. (2007) Ultradeep bisulfite sequencing analysis of DNA methylation patterns in multiple gene promoters by 454 sequencing. *Cancer Res.*, **67**, 8511–8518.
  27. Khulan, B., Thompson, R.F., Ye, K., Fazzari, M.J., Suzuki, M., Stasiak, E., Figueroa, M.E., Glass, J.L., Chen, Q., Montagna, C. *et al.* (2006) Comparative isoschizomer profiling of cytosine methylation: the HELP assay. *Genome Res.*, **16**, 1046–1055.
  28. Ibrahim, A.E., Thorne, N.P., Baird, K., Barbosa-Morais, N.L., Tavaré, S., Collins, V.P., Wyllie, A.H., Arends, M.J. and Brenton, J.D. (2006) MMAPS: an optimized array-based method for assessing CpG island methylation. *Nucleic Acids Res.*, **34**, e136.
  29. Lucito, R., Healy, J., Alexander, J., Reiner, A., Esposito, D., Chi, M., Rodgers, L., Brady, A., Sebat, J., Troge, J. *et al.* (2003) Representational oligonucleotide microarray analysis: a high-resolution method to detect genome copy number variation. *Genome Res.*, **13**, 2291–2305.
  30. Naume, B., Zhao, X., Synnæstvedt, M., Borgen, E., Russnes, H. G., Lingjærde, O.C., Strømberg, M., Wiedswang, G., Kvalheim, G., Kåresen, R. *et al.* (2007) Presence of bone marrow micrometastasis is associated with different recurrence risk within molecular subtypes of breast cancer. *Mol. Oncology*, **1**, 160–171.
  31. Bolstad, B.M., Irizarry, R.A., Astrand, M. and Speed, T.P. (2003) A comparison of normalization methods for high density oligonucleotide array data based on variance and bias. *Bioinformatics*, **19**, 185–193.
  32. R Development Core Team. (2007) R: A Language and Environment for Statistical Computing. *R Foundation for Statistical Computing*. Vienna, Austria.
  33. Benjamini, Y. and Hochberg, Y. (1995) Controlling the false discovery rate: a practical and powerful approach to multiple testing. *J. Roy. Stat. Soc. Ser. B*, **57**, 289–300.
  34. Pollard, K., Dudoit, S. and van der Laan, M.J.U.C. (2004) Multiple testing procedures: r multtest package and applications to genomics. *Berkeley Div Biostat Working Paper Ser.* 164.
  35. Van Rossum, G. and Drake, F.L. Jr. (2003) *The Python Language Reference Manual*. Network Theory Ltd. UK. p. 144.
  36. Li, L.C. and Dahiya, R. (2002) MethPrimer: designing primers for methylation PCRs. *Bioinformatics*, **18**, 1427–1431.
  37. Gebhard, C., Schwarzfischer, L., Pham, T.H., Schilling, E., Klug, M., Andreessen, R. and Rehli, M. (2006) Genome-wide profiling of CpG methylation identifies novel targets of aberrant hypermethylation in myeloid leukemia. *Cancer Res.*, **66**, 6118–6128.
  38. Costello, J.F., Smiraglia, D.J. and Plass, C. (2002) Restriction landmark genome scanning. *Methods*, **27**, 144–149.
  39. Chotai, K.A. and Payne, S.J. (1998) A rapid, PCR based test for differential molecular diagnosis of Prader-Willi and Angelman syndromes. *J. Med. Genet.*, **35**, 472–475.
  40. Yamada, Y., Watanabe, H., Miura, F., Soejima, H., Uchiyama, M., Iwasaka, T., Mukai, T., Sakaki, Y. and Ito, T. (2004) A comprehensive analysis of allelic methylation status of CpG islands on human chromosome 21q. *Genome Res.*, **14**, 247–266.
  41. Sutherland, E., Coe, L. and Raleigh, E.A. (1992) McrBC: a multisubunit GTP-dependent restriction endonuclease. *J. Mol. Biol.*, **225**, 327–348.
  42. Frommer, M., McDonald, L.E., Millar, D.S., Collis, C.M., Watt, F., Grigg, G.W., Molloy, P.L. and Paul, C.L. (1992) A genomic sequencing protocol that yields a positive display of 5-methylcytosine residues in individual DNA strands. *Proc. Natl Acad. Sci. USA*, **89**, 1827–1831.
  43. Maeta, Y., Shiota, G., Okano, J. and Murawaki, Y. (2005) Effect of promoter methylation of the p16 gene on phosphorylation of retinoblastoma gene product and growth of hepatocellular carcinoma cells. *Tumour Biol.*, **26**, 300–305.
  44. Omura, N., Li, C.P., Li, A., Hong, S.M., Walter, K., Jimeno, A., Hidalgo, M. and Goggins, M. (2008) Genome-wide profiling of methylated promoters in pancreatic adenocarcinoma. *Cancer Biol. Ther.*, **7**, 1146–1156.
  45. Sato, N., Fukushima, N., Chang, R., Matsubayashi, H. and Goggins, M. (2006) Differential and epigenetic gene expression profiling identifies frequent disruption of the RELN pathway in pancreatic cancers. *Gastroenterology*, **130**, 548–565.
  46. Imoto, I., Izumi, H., Yokoi, S., Hosoda, H., Shibata, T., Hosoda, F., Ohki, M., Hirohashi, S. and Inazawa, J. (2006) Frequent silencing of the candidate tumor suppressor PCDH20 by epigenetic mechanism in non-small-cell lung cancers. *Cancer Res.*, **66**, 4617–4626.
  47. Strathdee, G., Holyoake, T.L., Sim, A., Parker, A., Oscier, D.G., Melo, J.V., Meyer, S., Eden, T., Dickinson, A.M., Mountford, J.C. *et al.* (2007) Inactivation of HOXA genes by hypermethylation in myeloid and lymphoid malignancy is frequent and associated with poor prognosis. *Clin. Cancer Res.*, **13**, 5048–5055.
  48. Waha, A., Guntner, S., Huang, T.H., Yan, P.S., Arslan, B., Pietsch, T., Wiestler, O.D. and Waha, A. (2005) Epigenetic silencing of the protocadherin family member PCDH-gamma-A11 in astrocytomas. *Neoplasia*, **7**, 193–199.
  49. Ying, J., Gao, Z., Li, H., Srivastava, G., Murray, P.G., Goh, H.K., Lim, C.Y., Wang, Y., Marafioti, T., Mason, D.Y. *et al.* (2007) Frequent epigenetic silencing of protocadherin 10 by methylation in multiple haematologic malignancies. *Br. J. Haematol.*, **136**, 829–832.
  50. He, H., Jazdzewski, K., Li, W., Liyanarachchi, S., Nagy, R., Volinia, S., Calin, G.A., Liu, C.G., Franssila, K., Suster, S. *et al.* (2005) The role of microRNA genes in papillary thyroid carcinoma. *Proc. Natl Acad. Sci. USA*, **102**, 19075–19080.
  51. Hicks, D.G., Yoder, B.J., Short, S., Tarr, S., Prescott, N., Crowe, J.P., Dawson, A.E., Budd, G.T., Sizemore, S., Cicek, M. *et al.* (2006) Loss of breast cancer metastasis suppressor 1 protein expression predicts reduced disease-free survival in subsets of breast cancer patients. *Clin. Cancer Res.*, **12**, 6702–6708.
  52. Utikal, J., Gratchev, A., Muller-Moliniet, I., Oerther, S., Kzhyshkowska, J., Arens, N., Grobholz, R., Kannookadan, S. and Goerd, S. (2006) The expression of metastasis suppressor MIM/MTSS1 is regulated by DNA methylation. *Int. J. Cancer*, **119**, 2287–2293.
  53. Wang, Y., Liu, J., Smith, E., Zhou, K., Liao, J., Yang, G.Y., Tan, M. and Zhan, X. (2007) Downregulation of missing in metastasis gene (MIM) is associated with the progression of missing in bladder transitional carcinomas. *Cancer Invest.*, **25**, 79–86.
  54. Tryndyak, V., Kovalchuk, O. and Pogribny, I.P. (2006) Identification of differentially methylated sites within unmethylated DNA domains in normal and cancer cells. *Anal. Biochem.*, **356**, 202–207.
  55. Agathangelou, A., Honorio, S., Macartney, D.P., Martinez, A., Dallol, A., Rader, J., Fullwood, P., Chauhan, A., Walker, R., Shaw, J.A. *et al.* (2001) Methylation associated inactivation of RASSF1A from region 3p21.3 in lung, breast and ovarian tumours. *Oncogene*, **20**, 1509–1518.

56. Brenner,A.J., Paladugu,A., Wang,H., Olopade,O.I., Dreyling,M.H. and Aldaz,C.M. (1996) Preferential loss of expression of p16(INK4a) rather than p19(ARF) in breast cancer. *Clin. Cancer Res.*, **2**, 1993–1998.
57. Dammann,R., Yang,G. and Pfeifer,G.P. (2001) Hypermethylation of the cpG island of Ras association domain family 1A (RASSF1A), a putative tumor suppressor gene from the 3p21.3 locus, occurs in a large percentage of human breast cancers. *Cancer Res.*, **61**, 3105–3109.
58. Silva,J., Silva,J.M., Dominguez,G., Garcia,J.M., Cantos,B., Rodriguez,R., Larrondo,F.J., Provencio,M., Espana,P. and Bonilla,F. (2003) Concomitant expression of p16INK4a and p14ARF in primary breast cancer and analysis of inactivation mechanisms. *J. Pathol.*, **199**, 289–297.
59. Yekta,S., Shih,I.H. and Bartel,D.P. (2004) MicroRNA-directed cleavage of HOXB8 mRNA. *Science*, **304**, 594–596.
60. Fujino,T., Yamazaki,Y., Largaespada,D.A., Jenkins,N.A., Copeland,N.G., Hirokawa,K. and Nakamura,T. (2001) Inhibition of myeloid differentiation by Hoxa9, Hoxb8, and Meis homeobox genes. *Exp. Hematol.*, **29**, 856–863.
61. Knoepfler,P.S., Sykes,D.B., Pasillas,M. and Kamps,M.P. (2001) HoxB8 requires its Pbx-interaction motif to block differentiation of primary myeloid progenitors and of most cell line models of myeloid differentiation. *Oncogene*, **20**, 5440–5448.
62. Mattila,P.K., Salminen,M., Yamashiro,T. and Lappalainen,P. (2003) Mouse MIM, a tissue-specific regulator of cytoskeletal dynamics, interacts with ATP-actin monomers through its C-terminal WH2 domain. *J. Biol. Chem.*, **278**, 8452–8459.